

RAYLEIGH-TAYLOR INSTABILITY OF HIGH-VELOCITY CONDENSED-MATTER LINERS

S.F. Garanin, A.M. Buyko, V.B. Yakubov

Russian Federal Nuclear Center VNIIEF, Sarov, Russia

Abstract

Liner implosion driven by high magnetic pressures (high energy density ε) is of interest for generation and study of strong shock waves, generation of high magnetic fields, compression of magnetized plasma, and shockless compression of matter. Since $\varepsilon \sim \rho v^2$, it is important to ensure high ρ , which can be reached if the liner preserves its condensed state during implosion.

Liner acceleration can be accompanied by instabilities distorting the liner's shape and causing its growing non-uniformity. Among the potentially destructive instabilities one can accentuate the Rayleigh-Taylor (RT) instability.

We discuss the perturbation growth caused by the development of the RT instability during the liner implosion, the RT instability manifestation in some experiments, numerical simulation of the instability development and some methods of the RT instability mitigation.

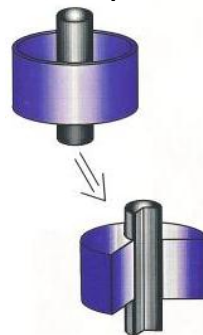
Introduction

The magnetic implosion of liners provides unique advantages for its application in experiments in the high energy density conditions:

- Liners are able to reach the velocities that significantly exceed those achieved when high explosives are used. At that the magnetic pressure becomes homogeneous also utterly instantaneously, which can help reaching better implosion symmetry;
- The liner acceleration rate and its final velocity can be controlled and varied in accordance with the experiment requirements;
- Magnetic field is able to support smooth liner acceleration without shock waves, which allows good control of the liner state and study of isentropic compression of materials.

Application of the liner implosion

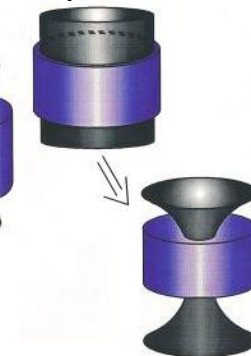
Shock Compression



Quasi-Isentropic Compression



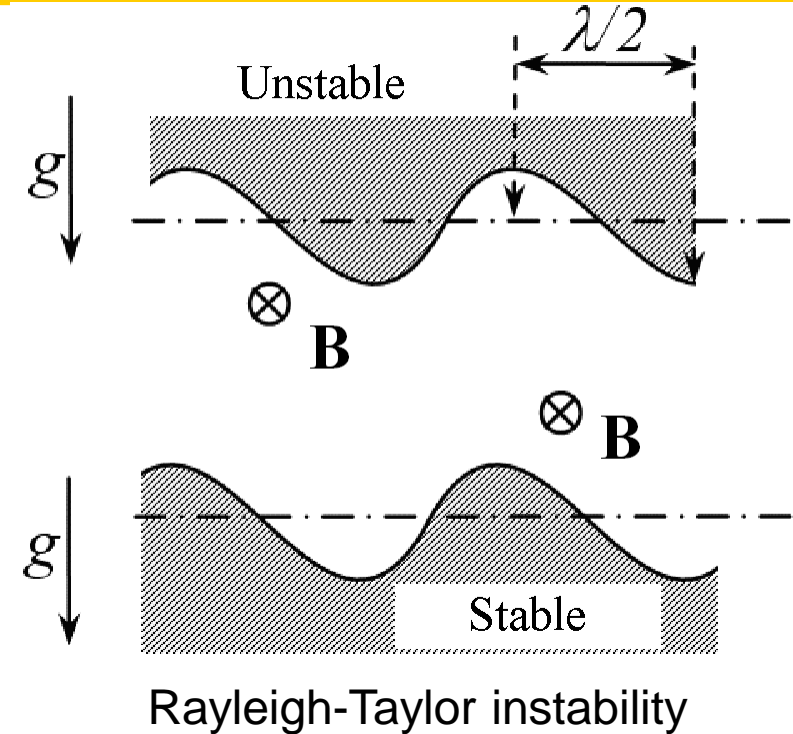
Hydrodynamic Compression



The liner characteristic important for applications is the value of dynamic pressure ρv^2 because this is the value that characterizes the energy density. Therefore, it is also important to have high ρ , which can be secured if during the implosion the liner remains in condensed state.

Introduction

Liner acceleration can be accompanied by instabilities distorting the liner's shape and causing its growing non-uniformity. Among the potentially destructive instabilities one can distinguish the Rayleigh-Taylor (RT) instability, which occurs when a low-density material drives a higher-density one, for example, when a magnetic field (zero-density matter) drives a dense liner.

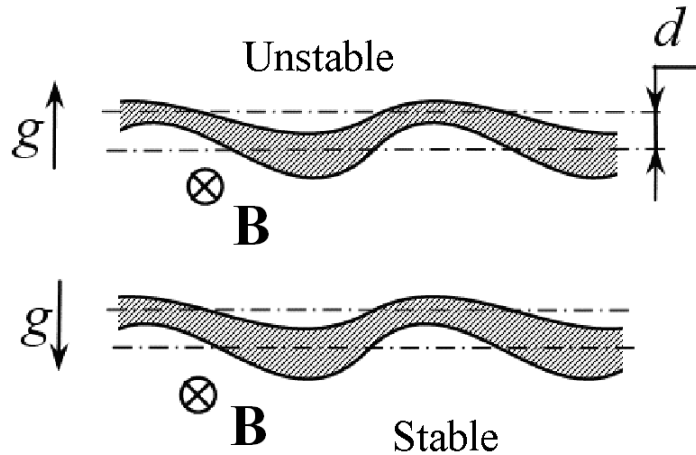


We consider the RT instability during the liner implosion, its manifestation in some experiments, numerical simulation of the instability development and some methods of the instability mitigation. In some sense this report can supplement the review report of A.Velikovich presented at the ICOPS-2015.

A.L. Velikovich, "Mitigation of Rayleigh-Taylor instability in high-energy density plasmas. A personal perspective," presented at the 42nd IEEE Int. Conf. on Plasma Science. Antalya, Turkey, 2015.

RT instability and perturbation growth. Assessment of sausage-mode instability effects. Linear stage

RT instability for an accelerated liner



In the linear theory the Fourier component of displacement of the fluid surface ζ (with wave vector k), changes in time as

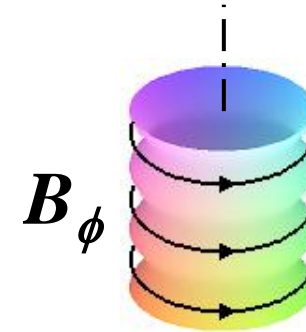
$$\zeta = \zeta_0 \exp(\gamma t + ikx) \quad \gamma^2 = \pm gk$$

wherein the plus corresponds to the case, when the fluid is supported by the magnetic field against the gravity force (instability), and the minus corresponds to the inverse, stable case (gravitational waves).

For a liner of thickness d driven by magnetic field B pressure the liner acceleration g is determined by the magnetic pressure

$$g = p_B / \rho d \quad p_B \equiv B^2 / 8\pi$$

Sausage instability $B \sim 1/r$



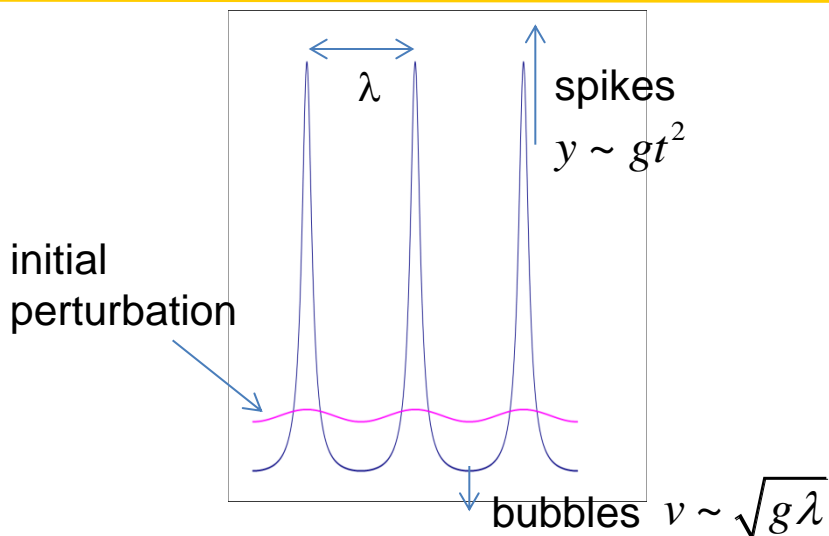
For small wavelengths $kr \gg 1$ the development of the "sausage" instability is reduced to the RT instability and has the increment

$$\sqrt{kg}$$

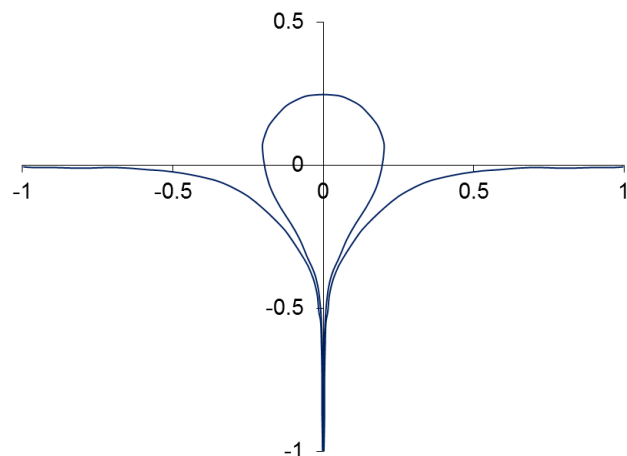
The liner material in this case plays the role of a heavy fluid, and the magnetic field, of a light fluid, while the role of the acceleration g will be played by

$$g_B = 2p_B / \rho r = B^2 / 4\pi\rho r = c_A^2 / r$$

The RT and sausage instabilities. Nonlinear stage



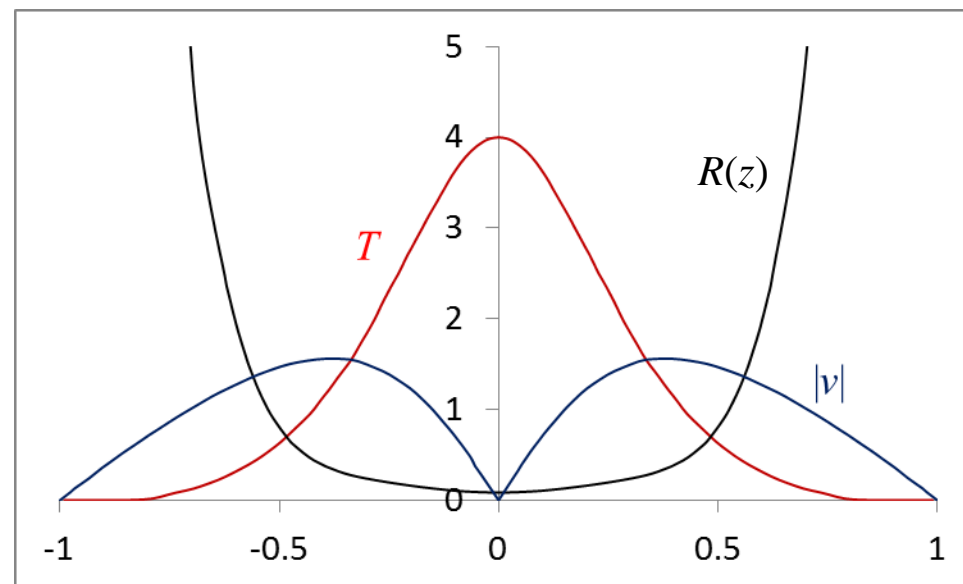
Development of periodical perturbations for the RT instability



$$x \sim gt^2$$

$$y \sim gt^2$$

Shape of the surface with self-similarity growth of localized perturbation



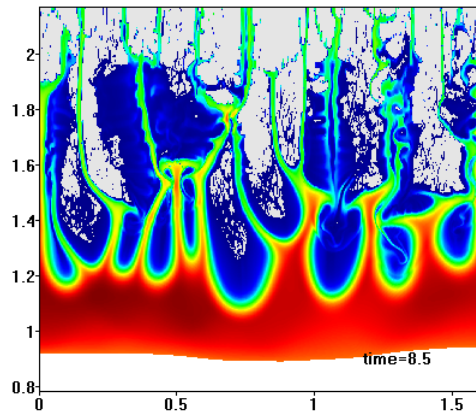
Waist shape in self-similar stage $R(z)$ and distributions along the waist length of temperature T and longitudinal velocity $|v|$

Waist radius R , matter density ρ , and temperature T depend on time as

$$R \sim t^{\gamma/(\gamma-1)} \quad \rho \sim t^{-2/(\gamma-1)} \quad T \sim t^{-2}$$

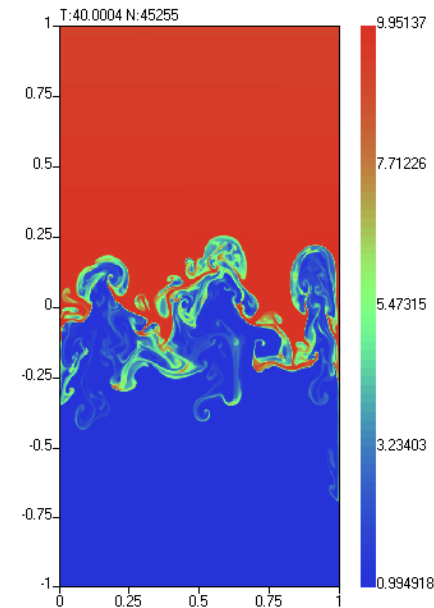
Turbulent stage of the MHD RT instability. Assessment of sausage-mode instability effects

The turbulent stage of the RT instability, just as the nonlinear stage, is characterized by the presence of bubbles and spikes. The bubbles and the spikes are located chaotically, and the bubbles coalesce as the instability develops, so the characteristic amplitudes a and wavelengths λ grow. $\lambda, a \sim$ some part of distance traveled with acceleration.



Distribution of liner density in the process of implosion

The turbulent flow associated with liner motion in an azimuthal magnetic field (z -pinch geometry) is 2D, since the magnetic field restrains the bending of magnetic field lines. 2D development of the RT instability for plane problem with constant g is an example of such flow.



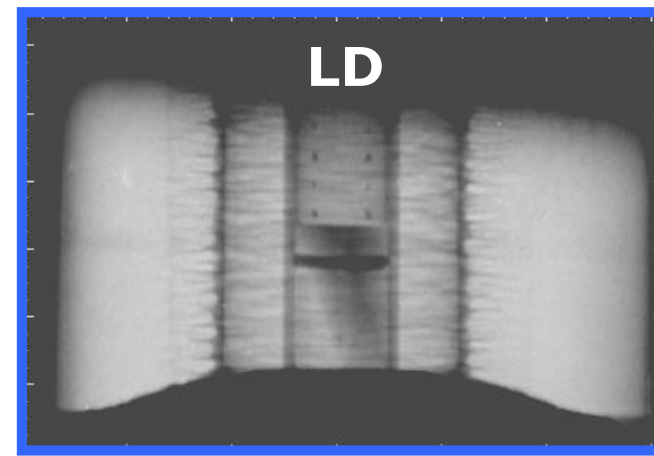
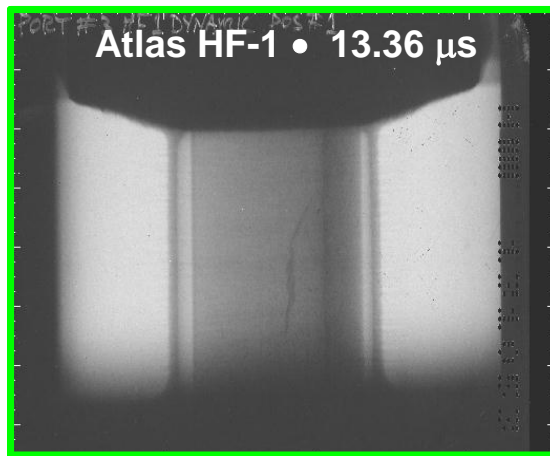
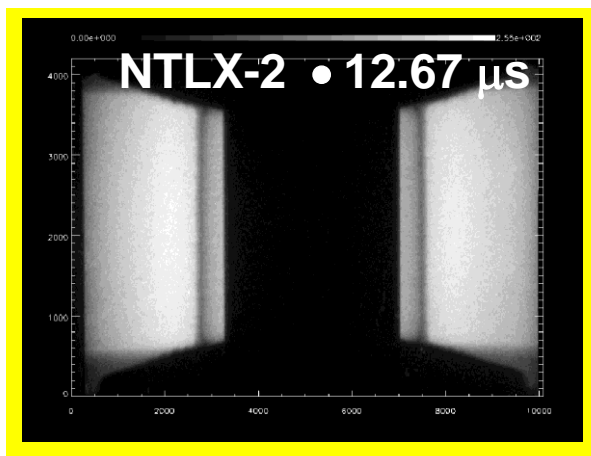
Distribution of density for the problem of 2D RT instability (g is constant and the initial density ratio is $\rho_H/\rho_L=10$)

The comparison of acceleration g , determining the RT instability mixing zone, and acceleration g_B , determining the sausage instability mixing zone, shows that their values relate as R/d

Instability development of condensed-matter liners in some experiments

Applications of condensed-matter liners in high-energy-density physics require liner velocities on the order of $1 \text{ cm}/\mu\text{s}$ and higher. Such velocities can be reached if liners are driven by megagauss magnetic fields, which cause melting and even vaporization and conversion to plasma of part of the liner (the skin layer), and respective loss of strength in this part. This provides conditions for the development of the RT instability in this liner region.

Similar experiments (initial liner radii were the same, thicknesses of the liners, the maximum currents, and the characteristic times for the currents differed not very much) conducted on the Shiva-Star (NTLX series) and on the Atlas (HF and LD series). Radiograms showed rather moderate or weak instability development in NTLX and HF and very strong instability development in LD.

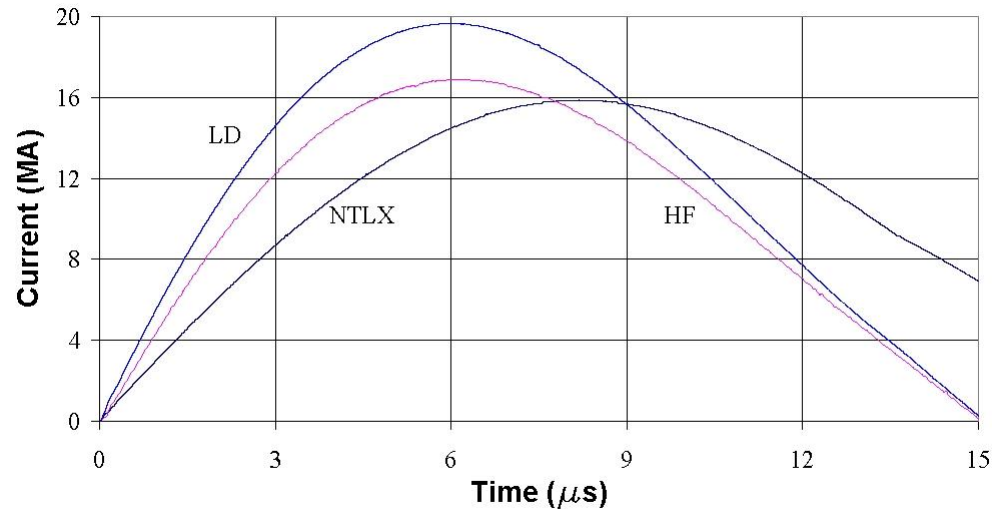


Radiography images in experiments: NTLX, HF, LD

Instability development of condensed-matter liners.

Problem Statement

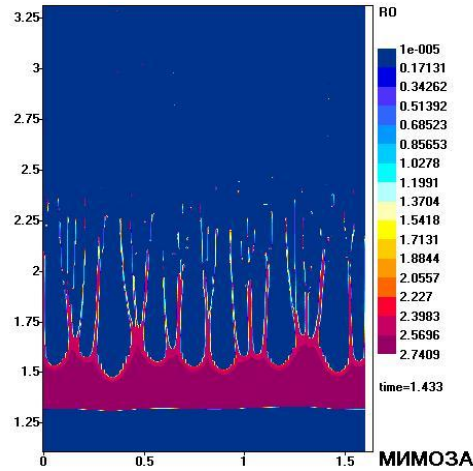
The NTLX, HF, and LD liners were aluminum, cylindrical; their initial radii were 5 cm. In the NTLX series, the liner was 0.1 cm thick, and in the HF and LD experiments, it was 0.13 cm thick.



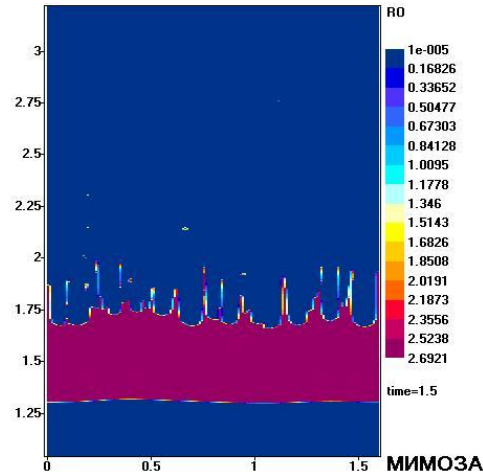
Current waveforms in the LD, NTLX, and HF series of experiments

The 2D r - z simulations were conducted on the Eulerian grid. In the computations, an equation of state in the Mie-Grueneisen form, resistive diffusion and Joule heating, and the material strength using the elastic-plastic model were taken into account.

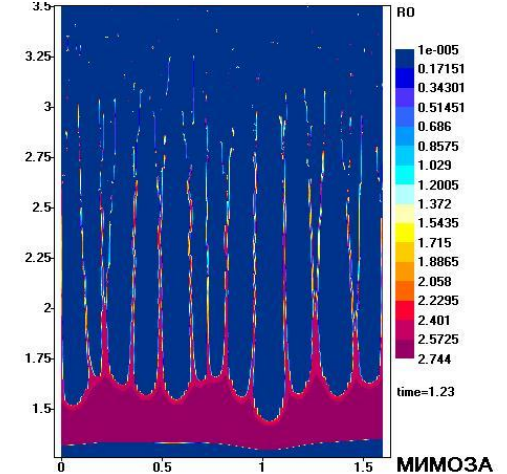
The initial perturbations were assumed to be random and to have characteristic values, which were determined by the mesh resolution.



NTLX



HF

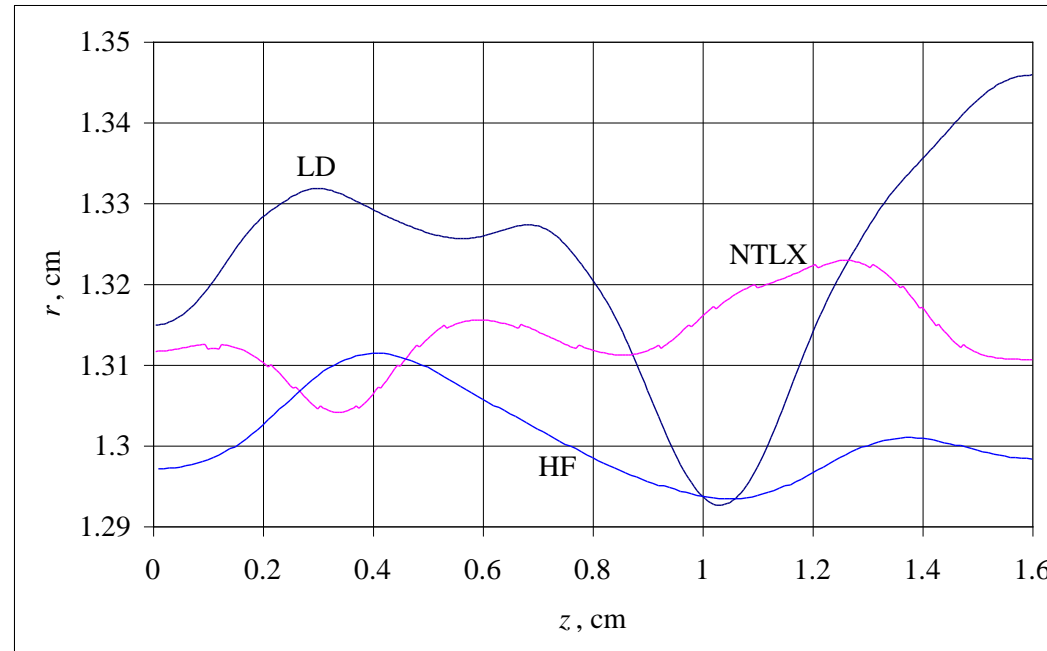


LD

Liner density plots, obtained in the NTLX, HF, and LD simulations at the times, corresponding to the liner internal-surface radius $R=1.3$ cm

The liner seems to be less perturbed in NTLX than in LD. NTLX still seems to be visibly more nonuniform than in the experiment. For the HF, the simulations reproduce more stable liner implosion than both in LD and NTLX, in agreement with the experiment.

2D MHD simulations of perturbation development



Shape of the liner internal surface, obtained in the simulations, when the liner internal-surface radius $R=1.3$ cm in the experiments: LD, NTLX, and HF

The perturbation amplitudes of the liner internal surface were 0.094 mm for NTLX, 0.265 mm for LD, and 0.09 mm for HF.

Instability development of condensed-matter liners in some experiments. Conclusions

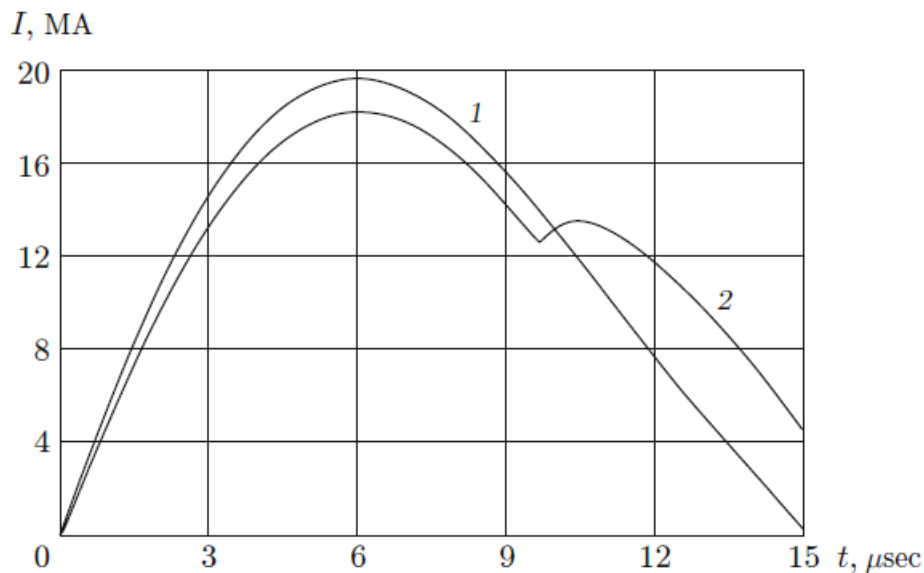
- 2D MHD simulations demonstrated that the HF and NTLX experimental conditions result in a smaller perturbation growth than those of the LD experiments, if the perturbation growth is quantified in terms of the perturbation development of the internal surface.
- A comparison of the simulated shape of the external liner surface for HF and LD showed that in the simulations, as well as in the experiments, the HF liner is weakly perturbed, whereas the LD liner is heavily distorted.
- However, for the LD and NTLX experiments, the shapes of the external liner surface remained qualitatively similar and rather heavily perturbed even at the refined mesh.

The techniques to suppress the development of RT instabilities

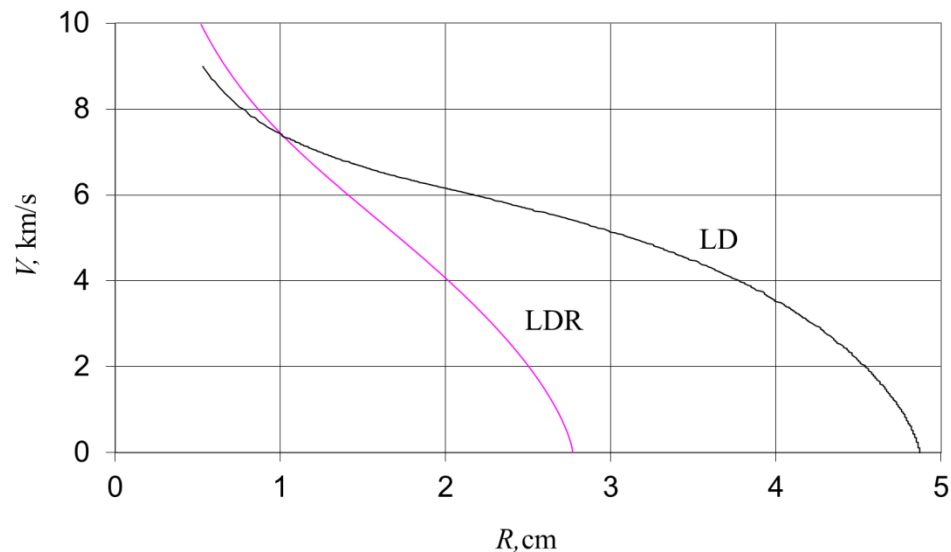
- Precision machining of liners to reduce the amplitude of their initial perturbations
- Reducing the aspect ratio R/d of the liner without changing its mass
- Liner machining to produce periodic perturbations of a certain wavelength such that the perturbations themselves have no time to destroy the liner during implosion but can efficiently suppress chaotic perturbations
- Collision of liners, as a result of which the target liner turns out to be less perturbed than the incident one
- The use of liner rotation and centrifugal acceleration induced by it
- Magnetic stabilization, in literature also referred to as the magnetic shear
- Coating of the metal liner surface with a plastic layer

The technique to suppress the development of RT instabilities. Effect of liner aspect ratio

It is proposed to reduce the initial liner radius (in comparison with LD experiments) from 5 to 3 cm. If we retain the mass of the liner, its thickness will be = 0.23 cm (instead of 0.13 cm). We call the proposed liner geometry LDR.



Current waveforms for the LD (1) and LDR (2)

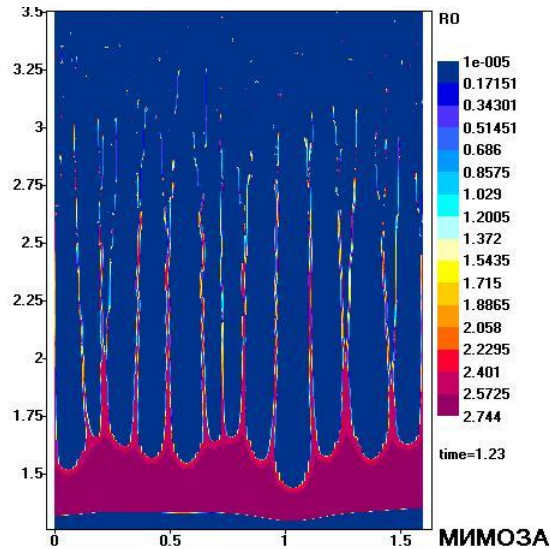


Dependence of the liner internal surface velocity on its radius for the LD and LDR

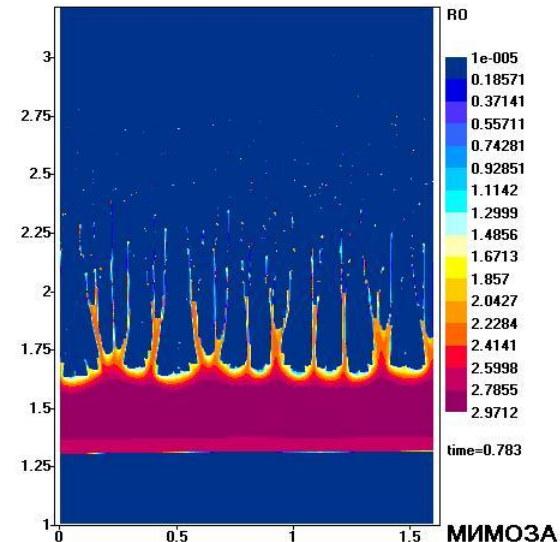
For the LDR the zone with a temperature above 0.1 eV (which approximately corresponds to the melting) at a liner radius of 2 cm is 37% of the liner mass, while for LD simulations, it is 44%.

The technique to suppress the development of RT instabilities. Effect of liner aspect ratio

2D simulations of liner implosion with the perturbation growth taken into account. Initial perturbations were assumed to be random with a characteristic magnitude determined by the resolution of the mesh.



LD



LDR

Liner density obtained in the LD and LDR simulations for the location of the inner liner surface $R=1.3$ cm

The perturbation amplitude of the liner inner surface is $a=0.265$ mm for LD and $a=0.026$ mm for LDR

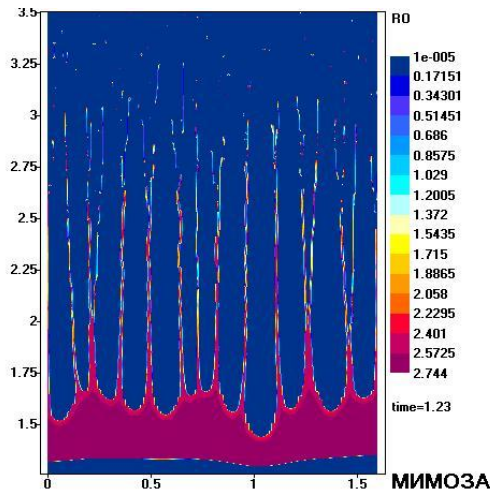
Development of liner instability in the presence of periodic perturbations

Considerations for choice of the wavelength λ^* and the initial amplitude a_0 of periodic perturbation:

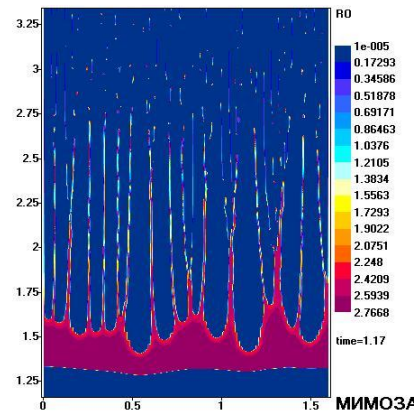
- 1) this perturbation itself, in the process of its development should not reach the inner liner surface,
- 2) the perturbation amplitude should be high enough such that the effect of this perturbation on the growth of chaotic perturbations is significant.

Based on the results of the 0D calculations, the initial parameters of the periodic (sinusoidal) perturbation:

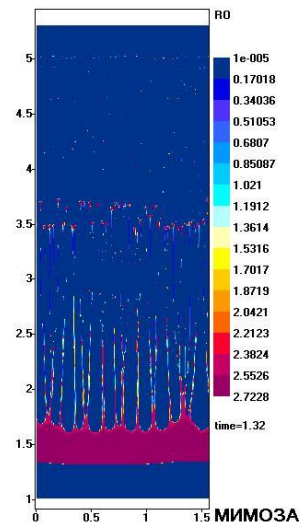
$$\lambda^* = 0.4 \text{ mm}, \quad a_0 = 0.13 \text{ mm}$$



LD



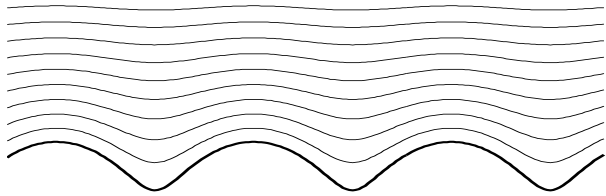
LDP



LDP1

Liner density obtained in the LD, LDP, and LDP1 simulations for the location of the inner liner surface $R=1.3 \text{ cm}$

The perturbation amplitude of the liner inner surface is $a=0.265 \text{ mm}$ for LD and $a=0.027 \text{ mm}$ for LDP. In the LDP simulation, as part of the liner mass is splashed due to the growth of the periodic perturbations, the liner acquires a higher velocity ($\approx 8.8 \text{ km/s}$) compared to LD (7.4 km/s). In the LDP1 simulation, the liner thickness was increased to 1.6 mm and the perturbation amplitude became $a=0.14 \text{ mm}$.

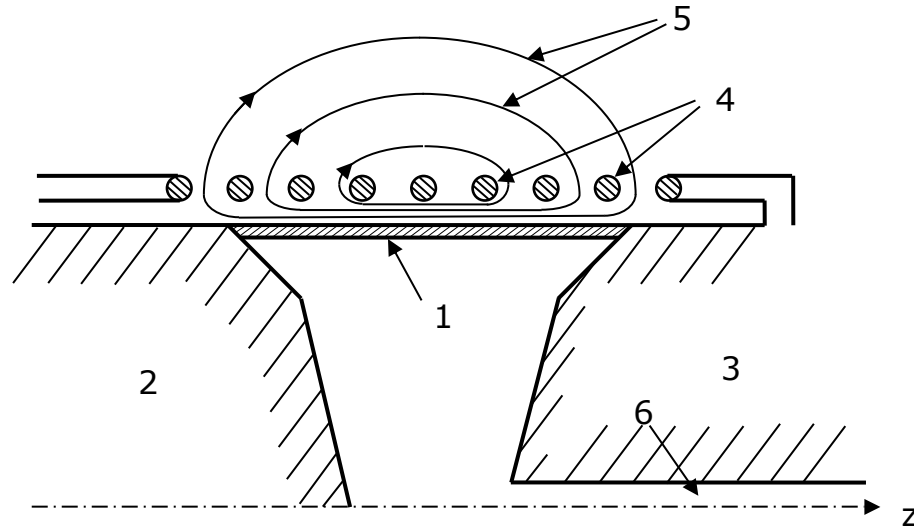


Magnetic field lines near a curved perfectly conducting surface

The field lines rarefy near the "valleys" on the liner surface and condense near the "peaks". The magnetic pressure $B^2/8\pi$ decreases near the valleys and increases near the peaks counteracting the growth of perturbations.

For perturbations with wave vector parallel to the magnetic field the increment of the perturbation growth is reduced.

It is possible to mitigate the RT instability changing the direction of the magnetic field during implosion, e.g. when the driving magnetic field is predominantly poloidal early during implosion, and predominantly azimuthal late in the implosion. This case can be implemented by placing a liner inside a coil and passing the current both through the coil and through the liner along the system axis. This system differs from the generally used z-pinch systems in that its return current conductor near the liner is replaced with a coil.



System geometry with an azimuthal and a poloidal magnetic field. 1: liner, 2 and 3: electrodes, 4: coil, 5: lines of the poloidal field, 6: diagnostic window.

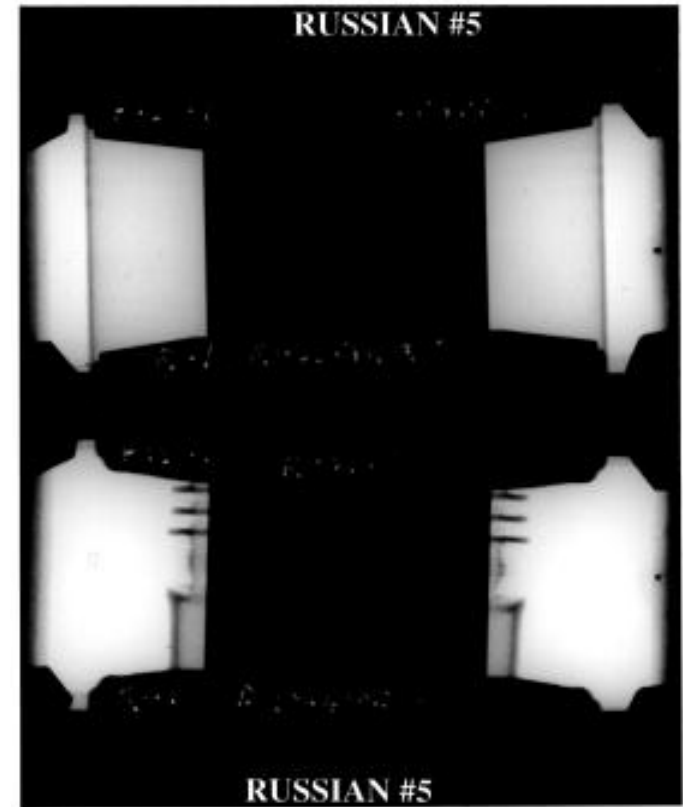
Magnetic stabilization of the RT instability. The joint LANL/VNIIEF experiment RUSSIAN-5

The (the z-pinch) aluminum liner was a straight circular cylinder with initial radius of 24 mm and a thickness of $d=0.5$ mm. One half of the liner had azimuthally symmetric sinusoidal perturbations machined on its outer surface. Their amplitude was 0.05 mm, and the wavelength was $\lambda=2$ mm. On the other half of the liner, machined perturbations had the same wavelength and amplitude, but the angle between their wave vector and the cylinder axis was 45° (screw perturbations). The azimuthally symmetric perturbations were to grow according to the classical RT law, because these perturbations do not deflect magnetic field lines and the magnetic stabilization effect does not work for them. However, the growth of the screw perturbations should be completely suppressed, because the criterion of complete suppression

$$\lambda < \lambda_{cr} = 4\pi d \cos^2 \theta$$

is fulfilled with a double margin, $\lambda_{cr}=4$ mm.

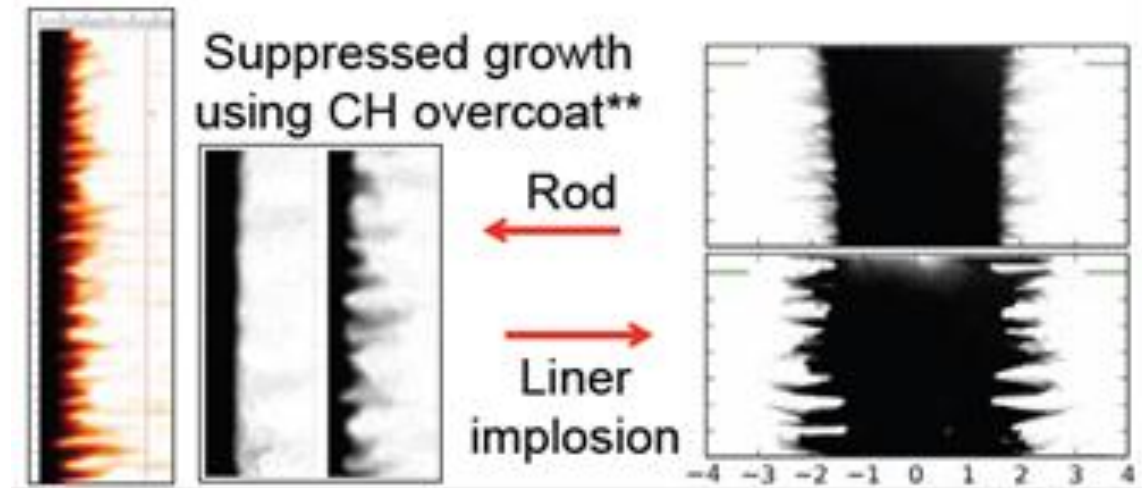
The azimuthally symmetric perturbations have grown from the amplitude, which was 10 times smaller than d , to the amplitude, which is several times larger than d . The other half of the liner (with screw perturbations) does not display any significant growth of perturbations.



Radiograms of liner in the initial position and at the time, when the liner radius decreases by a factor of ~ 1.5

Mitigation of RT instability growth using CH overcoat of the metal liner surface

Liner experiments on Z facility at SNL, USA, demonstrated that the development of magnetic RT instability can be suppressed if external surface of the liner is coated with relatively thick ($\sim 70 \mu\text{m}$) layer of insulator



Suppression of the sausage and RT instabilities if rods and liners using overcoat of plastic CH layer

Simplifications to study the development of RT instabilities are possible for small perturbations when one can use linear analysis when studying special cases and geometries, like the development of periodic perturbations and perturbations having no characteristic dimension (e.g. localized perturbations). In real cases fast non-linear development of short-wavelength perturbations results in the turbulization of the mixing zone at the interface between the magnetic field and the liner. In this case, MHD simulations represent an efficient tool for studying the development of instabilities.

Experiments show that even close drive conditions may lead to disparate liner states with different degrees of liner distortion. For example, in the LD, HF, and NTLX experiments with similar conditions, the radiography images obtained in HF and NTLX demonstrated a comparatively stable motion of the liner, while the radiographs in LD showed that the outer surface of the liner was severely distorted by the growth of perturbations. 2D numerical simulations of the liner implosion in the LD, HF, and NTLX experiments suggest that the experimental conditions in HF and NTLX indeed lead to a smaller growth of perturbations compared with LD.

To improve the performance of liner implosion, the techniques are explored which can mitigate the development of RT instabilities. These techniques include:

- reducing the aspect ratio R/d of the liner without changing its mass,
- liner machining to produce periodic perturbations such that the perturbations themselves have no time to destroy the liner during implosion but can suppress chaotic perturbations,
- magnetic stabilization, in literature also referred to as the magnetic shear,
- collision of liners, as a result of which the target liner turns out to be less perturbed than the incident one,
- the use of liner rotation and centrifugal acceleration induced by it,
- coating of the metal liner surface with a plastic layer.

References

1. R.E. Reinovsky, et al., Proc. IX Int. Conf. Megagauss Magnetic Field Generation and Related Topics, Moscow-St.-Petersburg, 2002. p. 696
2. A.L. Velikovich, "Mitigation of Rayleigh-Taylor instability in high-energy density plasmas. A personal perspective," presented at the 42nd IEEE Int. Conf. on Plasma Science. Belek, Antalya, Turkey, 2015
3. G.I. Taylor, Proc. Roy. Soc. London, vol. A 201, p. 192, 1950
4. E.G. Harris, Phys. Fluids, vol. 5, p. 1057, 1962
5. S.F. Garanin. Physical processes in the MAGO/MTF systems. Los Alamos, LA-UR-13-29094, 2013
6. S.F. Garanin, et al., Problems of high energy density physics. Proc. Int. Conf. XII Khariton Scientific Talks. Sarov. RFNC-VNIIEF, 2010. p. 235
7. W.L. Atchison, et al., Proc. IX Int. Conf. Megagauss Magnetic Field Generation Related Topics. Moscow-St.-Petersburg, 2002. p. 710, 2004
8. A.M. Buyko, et al., IEEE Trans. Plasma Science, vol. 36, p. 4, 2008
9. A.M. Buyko, et al., J. Appl. Mech. Tech. Phys., vol. 50, p. 361, 2009
10. K.J. Peterson, et al., Phys. Rev. Lett., vol. 112, p. 135002, 2014
11. B.G. Anderson, et al., Dig. Tech. Papers, Pulsed Power Plasma Science. Las Vegas, Nevada, p. 354, 2001